Available online at www.sciencedirect.com
SCIENCE DIRECT®
ELSEVIER
International Journal of Solids and Structures 42 (2005) 6566–6585
INTERNATIONAL JOURNAL OF SOLIDS and STRUCTURES
www.elsevier.com/locate/ijsolstr

Elastic and elastic–plastic singular fields around a crack-tip in particulate-reinforced composites with progressive debonding damage

Keiichiro Tohgo *, Takanori Itoh

Department of Mechanical Engineering, Shizuoka University, 3-5-1, Johoku, Hamamatsu 432-8561, Japan

Received 30 July 2004; received in revised form 18 April 2005
Available online 6 June 2005

Abstract

This paper deals with elastic and elastic–plastic singular fields around a crack-tip in particulate-reinforced composites with debonding damage of particle-matrix interface. Numerical analyses are carried out on a crack-tip field in elastic-matrix and elastic–plastic-matrix composites reinforced with elastic particles, using a finite element method developed based on an incremental damage theory of particulate-reinforced composites. A particle volume fraction and interfacial strength between particles and matrix of the composites are parametrically changed. In the elastic-matrix composites, a unique elastic singular field is created on the complete damage zone in the vicinity of a crack-tip in addition to the conventional elastic singular field on the no damage zone. The macroscopic stress level around a crack-tip is reduced by the debonding damage while the microscopic stress level of the matrix remains unchanged. In the elastic–plastic-matrix composites, the damage zone develops in addition to the plastic zone due to matrix plasticity, and both the macroscopic and microscopic stress revels around a crack-tip are reduced by the debonding damage. It is concluded from the numerical results that the toughening due to damage could be expected in the elastic–plastic-matrix composites, while it is questionable in the elastic-matrix composites.

Keywords: Particulate-reinforced composites; Debonding damage; Crack-tip field; Fracture toughness; Finite element analysis; Incremental damage theory

* Corresponding author. Tel./fax: +81 53 478 1027.
E-mail address: tmktoug@ipc.shizuoka.ac.jp (K. Tohgo).

0020-7683/$ - see front matter © 2005 Elsevier Ltd. All rights reserved.
doi:10.1016/j.ijsolstr.2005.04.013

1. Introduction

The technique to improve mechanical performance of materials by dispersing particles in a matrix has been applied to ceramic-matrix, metal-matrix and polymer-matrix composites, and these materials are called particulate-reinforced composites. In particulate-reinforced composites, a variety of damage modes such as fracture of particles, interfacial debonding between particles and matrix, and cracking in matrix develop from an early stage of deformation under monotonic and cyclic loads. The dominant damage mode depends on the relative strength of the particles, matrix and interface, as well as on the external loading mode. Influence of debonding or cracking damage on the stress–strain relation under uniaxial tension, tensile strength and fracture toughness was investigated on a variety of composites (Bayha et al., 1992; Llorca et al., 1993; Whitehouse and Clyne, 1993; Caceres and Griffiths, 1996; Kiser et al., 1996; Hartingsveldt and Aartsen, 1989; Tohgo et al., 1998; Tohgo et al., 1998). According to the results obtained by these investigations, progress of damage reduces the tensile strength while enhances the fracture toughness. If the mechanism of toughening due to damage were made clear, this knowledge would be useful in the material design of particulate-reinforced composites.

When we consider the damage around a crack-tip in elastic-particulate-reinforced composites, the situation is different between elastic-matrix composites such as ceramic-matrix composites and elastic–plastic-matrix composites such as polymer-matrix or metal-matrix composites. In the elastic-matrix composites, the influence of damage on the fracture toughness is obvious as the damage progresses under elastic state. On the other hand, in the elastic–plastic-matrix composites, a role of damage on toughening is ambiguous because both the damage and plastic deformation of the matrix develop around a crack-tip.

The similar problem can be seen in the microcrack toughening of ceramics. The effects of microcracks around a main crack in elastic homogeneous materials were investigated based on the continuum damage mechanics approach (Evans and Faver, 1984; Charalambides and McMeeking, 1987; Hutchinson, 1987; Ortiz, 1987) and the crack-interaction approach (Rose, 1986a; Hori and Nemat-Nasser, 1987; Shum and Hutchinson, 1990; Kachanov et al., 1990; Gong, 1995; Brencich and Carpinteri, 2000). In the former approach, the microcracking zone is regarded as a damage zone around a crack-tip obtained by the calculation based on the appropriate constitutive relation describing the deformation of continuum with progressive cracking damage. The model predicts the stress reduction around a crack-tip due to the microcracking damage, and this suggests the toughening due to crack shielding. However, it has been pointed out that this contribution is reduced by the toughness degradation of the microcracked material (Rose, 1986b; Ortiz, 1988). In the latter approach, the reduction of stress intensity of a main crack due to microcracks in the damage zone is estimated based on the interaction effects between the main crack and microcracks. Although the reduction of stress intensity leads to the toughening, the result has been obtained under the assumption of no interaction among microcracks. The toughening of ceramics due to microcracking damage is true to some extent, but the essence of its mechanism is still unknown. In the present study, the influence of debonding damage on a crack-tip field and toughness in particulate-reinforced composites has been studied based on the continuum damage mechanics approach.

The influence of progressive damage on the stress–strain relationship of particulate-reinforced composites was studied with two schemes. Finite element analysis for a unit cell containing one particle in a matrix was widely applied to the fracture or debonding of particles (Needleman, 1987; Bao, 1992; Finot et al., 1994; Brockenbrough and Zok, 1995; Llorca and Segurado, 2004). However, because it is assumed in the unit-cell analysis that all particles are in the same stage of damage process, we can not obtain the overall stress–strain response of the realistic composites containing intact particles and damaged particles. To overcome this problem, some modifications were proposed; for examples, the damage cell model (Bao, 1992) and multi-particles cell model (Llorca and Segurado, 2004). On the other hand, some micromechanics-based models were developed. Tohgo and Chou (1996) and Tohgo and Weng (1994) proposed an incremental damage theory of particulate-reinforced composites taking account of the plasticity of the matrix and the progressive debonding damage of particles based on the Eshelby's equivalent inclusion method

(Eshelby, 1957) and Mori–Tanaka's mean field concept (Mori and Tanaka, 1973). This theory was also extended to the progressive cracking damage of particles in particulate-reinforced composites (Cho et al., 1997; Tohgo and Cho, 1999). Chen et al. (2003) developed the constitutive relation of particulate-reinforced viscoelastic-matrix composites with progressive debonding damage based on the same scheme. Matous (2003) presented the constitutive relation of particulate-reinforced composites with debonding damage based on the transformation field analysis (Dvorak and Benveniste, 1992) and imperfect interface model (Hashin, 1991) and applied it to numerical simulation of damage evolution in glass-elastomer composites. The micromechanics-based models have the advantage of easy implementation into a finite element method. Tohgo et al. (2001) introduced their damage theory into a finite element method, and carried out damage analysis of a crack-tip field in glass-particle-reinforced Nylon 66 composites. From the experimental and numerical results, it was found that in glass-particle-reinforced Nylon 66 composites the debonding damage reduces the tensile strength and enhances the fracture toughness.

In this paper, numerical analyses are carried out on a crack-tip field in elastic-matrix and elastic–plastic-matrix composites reinforced with elastic particles using the finite element method based on the incremental damage theory of particulate-reinforced composites. A particle volume fraction and interfacial strength between particles and matrix of the composites are parametrically changed. On a crack-tip field in particulate-reinforced composites, microscopic stress/strain fields of the particles and matrix are obtained in addition to macroscopic stress/strain fields. The mechanism of toughening due to the debonding damage is discussed based on the macroscopic and microscopic stress fields around a crack-tip.

2. Incremental damage theory

Tohgo and Chou (1996) developed an incremental damage theory, which describes the plasticity of a matrix and the progressive debonding damage of particles in particulate-reinforced composites, based on the Eshelby's equivalent inclusion method (Eshelby, 1957) and Mori and Tanaka's mean field concept (Mori and Tanaka, 1973). Here, the incremental damage theory of particulate-reinforced composites is briefly explained. For the present theory, the limitations and comparison with other theories were already discussed in references (Tohgo and Chou, 1996; Tohgo and Weng, 1994). The incremental constitutive relation ($d\varepsilon_{ij} - d\sigma_{ij}$ relation) is described by the form decomposed into the hydrostatic part ($d\varepsilon_{kk} - d\sigma_{kk}$ relation) and the deviatric part ($d\varepsilon'_{ij} - d\sigma'_{ij}$ relation). $d\sigma_{ij}$ and $d\varepsilon_{ij}$ are incremental total stress and strain, $(1/3)d\sigma_{kk}$, $(1/3)d\varepsilon_{kk}$ and $d\sigma'_{ij}$, $d\varepsilon'_{ij}$ are their hydrostatic and deviatric parts, respectively. The incremental total stress and strain are given by

$$d\sigma_{ij} = d\sigma'_{ij} + \frac{1}{3}d\sigma_{kk}\delta_{ij}, \quad d\varepsilon_{ij} = d\varepsilon'_{ij} + \frac{1}{3}d\varepsilon_{kk}\delta_{ij} \tag{1}$$

where δ_{ij} is the Kronecker delta. In the composite system elastic spherical particles are homogeneously dispersed in an elastic–plastic matrix.

2.1. Properties of constituent materials

The elastic incremental stress–strain relation of the isotropic particle follows as

$$d\varepsilon_{kk} = \frac{1}{3\kappa_p}d\sigma_{kk}, \quad d\varepsilon'_{ij} = \frac{1}{2\mu_p}d\sigma'_{ij} \tag{2}$$

where κ_p and μ_p are the bulk modulus and shear modulus of the particle. The elastic behavior of the matrix is also taken to be isotropic with the moduli κ_0 and μ_0. κ_0, κ_p and μ_0, μ_p are related to the Young's moduli E_0, E_p and Poisson's ratios ν_0, ν_p by

$$\kappa_i = \frac{E_i}{3(1-2\nu_i)}, \quad \mu_i = \frac{E_i}{2(1+\nu_i)}, \quad i = 0 \text{ or } p \tag{3}$$

The elastic–plastic deformation of the matrix is described by the Prandtl–Ruess equation (the J2-flow theory), which is approximated by the following isotropic relation (Tohgo and Chou, 1996):

$$\mathrm{d}\varepsilon_{kk} = \frac{1}{3\kappa_0}\mathrm{d}\sigma_{kk}, \quad \mathrm{d}\varepsilon'_{ij} = \frac{1}{2\mu_0}\mathrm{d}\sigma'_{ij} \tag{4}$$

where

$$\mu'_0 = \frac{\mu_0}{1+\dfrac{3\mu_0}{H'}}, \quad \nu'_0 = \frac{\nu_0 + \dfrac{\mu_0}{H'}(1+\nu_0)}{1+2\dfrac{\mu_0}{H'}(1+\nu_0)} \tag{5}$$

and μ'_0 and ν'_0 are the tangent shear modulus and tangent Poisson's ratio of the matrix under elastic–plastic deformation (Berveiller and Zaoui, 1979). H' is the work-hardening ratio of the matrix:

$$H' = \frac{\mathrm{d}\sigma_e}{\mathrm{d}\varepsilon_e^{\mathrm{pl}}} \tag{6}$$

where

$$\sigma_e = \left(\frac{3}{2}\sigma'_{ij}\sigma'_{ij}\right)^{1/2}, \quad \mathrm{d}\varepsilon_e^{\mathrm{pl}} = \left(\frac{2}{3}\mathrm{d}\varepsilon_{ij}^{\mathrm{pl}}\mathrm{d}\varepsilon_{ij}^{\mathrm{pl}}\right)^{1/2} \tag{7}$$

Here σ_e and $\mathrm{d}\varepsilon_e^{\mathrm{pl}}$ are the von Mises' equivalent stress and incremental equivalent plastic strain, respectively, and $\mathrm{d}\varepsilon_{ij}^{\mathrm{pl}}$ is the incremental plastic strain. Eq. (4) is strictly valid in the case of monotonic proportional loading.

In the composite system the stress and strain of the particles and matrix are represented with the superscripts "p" and "0", respectively, and those of the composite are shown by symbols without superscript.

2.2. Incremental constitutive relation of composite with progressive debonding damage

The composite under consideration contains spherical particles with a finite concentration f_{p0} in a matrix. This composite is statistically homogeneous and macroscopically isotropic. Fig. 1 illustrates the states before and after incremental deformation of the composite in the damage process. Solid and open circles in the figure represent the intact particles and debonded particles, respectively. In the composite, the microscopic stresses/strains in the intact particles, damaged particles and matrix are generated due to the material heterogeneity, in addition to the overall macroscopic stress/strain. The process of debonding damage, namely the separation of particles from the matrix, in such a composite can be simulated by the following assumptions.

(1) The debonding of particles is controlled by the stress of the particles and the statistical behavior of the particle-matrix interfacial strength. Here, the particle stress is used because the interfacial stress is given as a function of the particle stress (Tandon and Weng, 1986).
(2) During debonding, the stress of the debonded particle is released and the site of the particle is regarded as a void.
(3) A volume fraction of the debonded particles turns into a void volume fraction, and progressive damage in the composite is expressed by a decrease in an intact particle volume fraction and an increase in a void volume fraction.

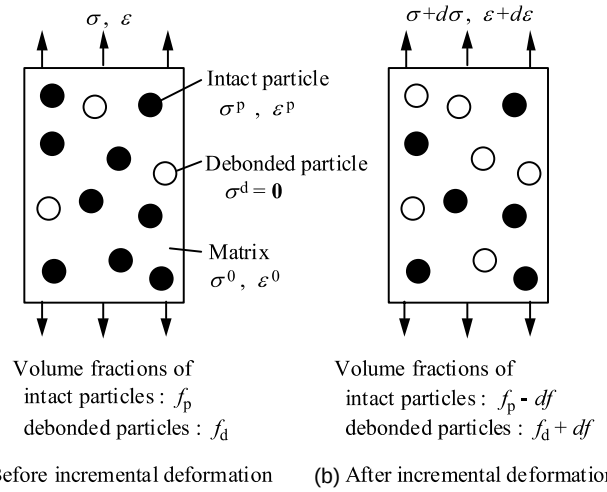

Fig. 1. The states of a composite undergoing damage process before and after incremental deformation. df_p is a volume fraction of the particles debonded in the incremental process.

There is limitation in the above assumption that the debonded particles are regarded as voids because the debonded particles can sustain the compressive stress. However, this is reasonable for the damage behavior under the triaxial tensile stress state as in a crack-tip field under mode I loading.

If the volume fraction of the particles to be debonded in the incremental process is denoted by df, the volume fractions of the intact particles and the damaged particles (voids) will change from f_p and f_d for the state before deformation (Fig. 1(a)) to $f_p - df$ and $f_d + df$ for the state after deformation (Fig. 1(b)), respectively. In order to describe the deformation and damage of the composite in this incremental process, the Eshelby's equivalent inclusion method and Mori and Tanaka's mean field concept were applied for the heterogeneous body containing the intact particles, voids and particles to be debonded. For this incremental deformation, the constitutive relation is given as follows:

$$d\varepsilon_{kk} = \frac{1}{3\kappa_t} d\sigma_{kk} + \frac{1}{3\kappa_d} \sigma^p_{kk} df \tag{8}$$

$$d\varepsilon'_{ij} = \frac{1}{2\mu_t} d\sigma'_{ij} + \frac{1}{2\mu_d} \sigma^{p\prime}_{ij} df \tag{9}$$

where

$$\kappa_t = \frac{\kappa_0(1-\alpha)A_h}{\{(1-\alpha)(1-f_p-f_d)+f_d\}\{\kappa_0+(\kappa_p-\kappa_0)\alpha\}+\kappa_0(1-\alpha)f_p} \tag{10}$$

$$\mu_t = \frac{\mu_0(1-\beta)A_d}{\{(1-\beta)(1-f_p-f_d)+f_d\}\{\mu_0+(\mu_p-\mu_0)\beta\}+\mu_0(1-\beta)f_p} \tag{11}$$

$$\kappa_d = \frac{\kappa_0(1-\alpha)A_h}{\kappa_0+(\kappa_p-\kappa_0)\alpha} \tag{12}$$

$$\mu_d = \frac{\mu_0(1-\beta)A_d}{\mu_0+(\mu_p-\mu_0)\beta} \tag{13}$$

and

$$A_h = (1 - f_p - f_d)\{\kappa_0 + (\kappa_p - \kappa_0)\alpha\} + f_p\kappa_p \tag{14}$$

$$A_d = (1 - f_p - f_d)\{\mu_0 + (\mu_p - \mu_0)\beta\} + f_p\mu_p \tag{15}$$

Here $(\mathrm{d}\sigma_{kk}, \mathrm{d}\sigma'_{ij})$ and $(\mathrm{d}\varepsilon_{kk}, \mathrm{d}\varepsilon'_{ij})$ are the incremental stress and strain of the composite, and $(\sigma^p_{kk}, \sigma^{p\prime}_{ij})$ denotes the current stress of the particles. With spherical particles and voids the constants α and β follow from Eshelby's relations (Eshelby, 1957):

$$\alpha = \frac{1}{3}\frac{1+\nu_0}{1-\nu_0}, \quad \beta = \frac{2}{15}\frac{4-5\nu_0}{1-\nu_0} \tag{16}$$

Incremental average stresses of the matrix and particles are given by

$$\mathrm{d}\sigma^0_{kk} = \frac{\kappa_0 + (\kappa_p - \kappa_0)\alpha}{A_h}(\mathrm{d}\sigma_{kk} + \sigma^p_{kk}\mathrm{d}f) \tag{17}$$

$$\mathrm{d}\sigma^{0\prime}_{ij} = \frac{\mu_0 + (\mu_p - \mu_0)\beta}{A_d}(\mathrm{d}\sigma'_{ij} + \sigma^{p\prime}_{ij}\mathrm{d}f) \tag{18}$$

$$\mathrm{d}\sigma^p_{kk} = \frac{\kappa_p}{A_h}(\mathrm{d}\sigma_{kk} + \sigma^p_{kk}\mathrm{d}f) \tag{19}$$

$$\mathrm{d}\sigma^{p\prime}_{ij} = \frac{\mu_p}{A_d}(\mathrm{d}\sigma'_{ij} + \sigma^{p\prime}_{ij}\mathrm{d}f) \tag{20}$$

Furthermore, incremental average strains of the matrix and particles are given by

$$\mathrm{d}\varepsilon^0_{kk} = \frac{\kappa_0 + (\kappa_p - \kappa_0)\alpha}{3\kappa_0 A_h}(\mathrm{d}\sigma_{kk} + \sigma^p_{kk}\mathrm{d}f) \tag{21}$$

$$\mathrm{d}\varepsilon^{0\prime}_{ij} = \frac{\mu_0 + (\mu_p - \mu_0)\beta}{2\mu_0 A_d}(\mathrm{d}\sigma'_{ij} + \sigma^{p\prime}_{ij}\mathrm{d}f) \tag{22}$$

$$\mathrm{d}\varepsilon^p_{kk} = \frac{1}{3A_h}(\mathrm{d}\sigma_{kk} + \sigma^p_{kk}\mathrm{d}f) \tag{23}$$

$$\mathrm{d}\varepsilon^{p\prime}_{ij} = \frac{1}{2A_d}(\mathrm{d}\sigma'_{ij} + \sigma^{p\prime}_{ij}\mathrm{d}f) \tag{24}$$

2.3. Cumulative probability of debonded particles

The Weibull distribution is modified to describe the cumulative volume ratio of the debonded particles to the total particles as follows:

$$P_d(\sigma^p_{\max}) = P_0\left[1 - \exp\left\{-\left(\frac{\sigma^p_{\max}}{S_0}\right)^m\right\}\right] \tag{25}$$

where $\sigma^p_{\max}$ is the maximum tensile stress of the particle and P_0, S_0 and m are the maximum damage ratio, scale parameter and shape parameter, respectively. As the parameter controlling the debonding damage, although the maximum tensile stress $\sigma^p_{\max}$ or the hydrostatic stress $\sigma^p_m(=(1/3)\sigma^p_{kk})$ of the particles can be used, $\sigma^p_{\max}$ is adopted here. The average interfacial strength is given by

$$\bar{\sigma}^p_{\max} = S_0\Gamma\left(1 + \frac{1}{m}\right) \tag{26}$$

where $\Gamma(\cdot)$ is the Gamma function. If an initial particle volume fraction is denoted by f_{p0}, as a cumulative volume fraction of the damaged particles is represented by $f_{p0}P_d$, the volume fraction of the particles to be debonded in the incremental deformation is given by

$$\mathrm{d}f = f_{p0}\frac{\mathrm{d}P_d}{\mathrm{d}\sigma^p_{\max}}\mathrm{d}\sigma^p_{\max} \tag{27}$$

2.4. Equivalent stress of the matrix in composite

In order to describe the matrix plasticity, we need to estimate the von Mises' equivalent stress of the matrix in a composite. In the composite, as the matrix deforms heterogeneously, the microscopic stress and von Mises' equivalent stress are not uniform but distributed in the matrix. On the other hand, the present theory gives the average microscopic stress of the matrix. Tohgo and Weng (1994) proposed the expression for the average von Mises' equivalent stress of the matrix taking account of the heterogeneous deformation in the composite. According to the theory, an initial equivalent stress σ^0_e of the matrix in the composite before plastic deformation and damage is given by

$$(\sigma^0_e)^2 = \frac{3\mu_0}{(1-f_{p0})}(2U - f_{p0}\sigma^p_{ij}\varepsilon^p_{ij}) - \frac{3\mu_0}{\kappa_0}(\sigma^0_m)^2 \tag{28}$$

where $\sigma^0_m(=(1/3)\sigma^0_{kk})$ is the average hydrostatic stress of the matrix. U is energy of a unit volume of the composite:

$$U = \frac{1}{2}\sigma_{ij}\varepsilon_{ij} \tag{29}$$

After the incremental deformation the equivalent stress of the matrix is estimated by $\sigma^0_e + \mathrm{d}\sigma^0_e$, where σ^0_e and $\mathrm{d}\sigma^0_e$ denote the current equivalent stress before the incremental deformation and its increment, respectively. In the numerical analysis σ^0_e is known and $\mathrm{d}\sigma^0_e$ is given by

$$\mathrm{d}\sigma^0_e = \frac{3\mu_0}{\sigma^0_e(1-f_p-f_d)}\left\{\mathrm{d}U - \mathrm{d}R - f_p\sigma^p_{ij}\mathrm{d}\varepsilon^p_{ij} + \frac{1}{2}\mathrm{d}f_p\sigma^p_{ij}\varepsilon^p_{ij}\right\} - \frac{3\mu_0}{\sigma^0_e\kappa_0}\sigma^0_m\mathrm{d}\sigma^0_m \tag{30}$$

where $\mathrm{d}U$ is incremental energy of the composite and $\mathrm{d}R$ is energy released by the debonding damage:

$$\mathrm{d}U = \sigma_{ij}\mathrm{d}\varepsilon_{ij} \tag{31}$$

$$\mathrm{d}R = \frac{1}{2}\sigma_{ij}\mathrm{d}\varepsilon^d_{ij} \tag{32}$$

where $\mathrm{d}\varepsilon^d_{ij}$ is the strain increment due to damage corresponding to the second terms in Eqs. (8) and (9).

If the matrix is in the elastic–plastic state, the elastic moduli μ_0 and ν_0 in all equations in Sections 2.2 and 2.4 reduce to their elastic–plastic counterparts μ'_0 and ν'_0, respectively.

In the deformation and damage behavior of particulate-reinforced composites, particle size is an important factor in addition to the particle volume fraction. However, the present model based on the Eshelby's equivalent inclusion method and Mori–Tanaka's mean field concept can not describe the influence of particle size on the elastic–plastic deformation. Although the influence of particle size on the debonding damage may be included in cumulative probability of debonded particles Eq. (25), there is no available data in literatures. Implementation of the size effect of particles into the model would be carried out as our future work.

3. Numerical procedure

3.1. Material properties and debonding properties

The Young's moduli and Poisson's ratios for the particles and matrix of the composites were given as follows:

$$E_0 = 500\sigma_0, \quad v_0 = 0.3 \tag{33}$$

$$E_p = 2500\sigma_0, \quad v_p = 0.17 \tag{34}$$

In the case of elastic–plastic-matrix composites, the equivalent stress vs. equivalent plastic strain relation for the matrix was expressed by

$$\sigma_e^0 = \sigma_0\left(1 + \frac{\varepsilon_e^{0p}}{\varepsilon_0}\right)^{0.1}, \quad \varepsilon_0 = \frac{\sigma_0}{E_0} \tag{35}$$

In the above relations, σ_0 is the reference stress of the matrix for the elastic-matrix composites or the yield stress of the matrix for the elastic–plastic-matrix composites. In Eq. (25), the maximum damage ratio and shape parameter were assigned as $P_0 = 1$ and $m = 8$, and the scale parameter S_0 was changed so that the average debonding strength $\bar{\sigma}^p_{\max}$ given by Eq. (26) was equal to $0.5\sigma_0$, $1.5\sigma_0$ and $2.5\sigma_0$. $P_0 = 1$ means that all particles in composites can be debonded.

By using the above material properties and debonding properties, several composites with different particle volume fractions and debonding properties were designed. Hereafter, the composite in which any damage does not develop during deformation is referred to as *perfect composite*, and the composite in which the debonding damage occurs with deformation is referred to as *composite with damage* or *damaged composite*. For the elastic-matrix composites, six kinds of composites were analyzed, where the particle volume fraction was varied in 10%, 20% and 30% for the perfect composites and the composites with damage of $\bar{\sigma}^p_{\max} = 2.5\sigma_0$. Fig. 2 shows the uniaxial stress–strain relations obtained by the damage theory for the composites with damage. The damage evolution is also shown by means of a volume fraction of the damaged particles (voids) for the right hand scale in Fig. 2. Numerical calculation was carried out under strain control with a strain increment of 0.003–0.004%. The stress–strain relations of the composites are linear before damage initiation, nonlinear during damage evolution and linear again after damage completion. In the

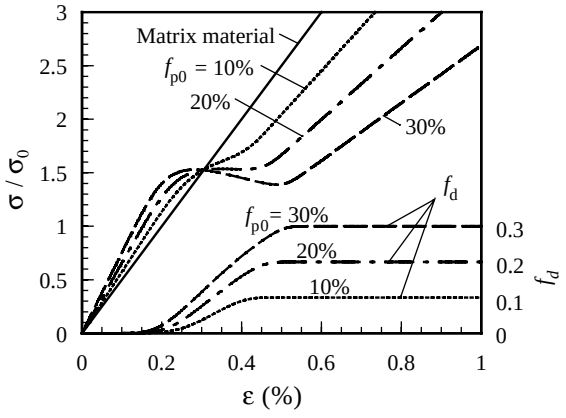

Fig. 2. Stress–strain relations and damage evolution under uniaxial tension for elastic-matrix composites.

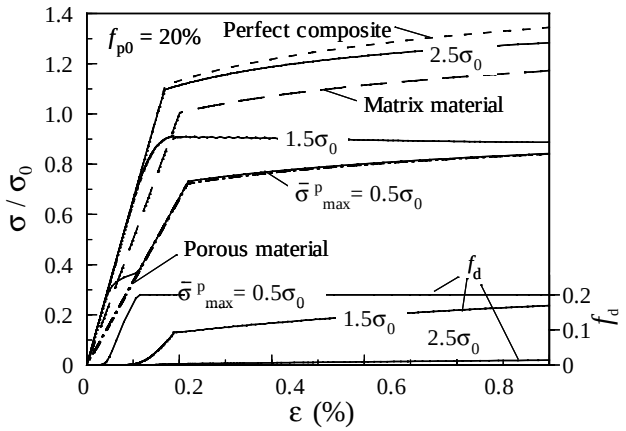

Fig. 3. Stress–strain relations and damage evolution under uniaxial tension for elastic–plastic-matrix composites.

composite with higher particle volume fraction, the influence of damage on the stress–strain relation is more remarkable, namely the stiffness is higher before damage initiation and lower after damage completion.

For the elastic–plastic-matrix composites, nine kinds of materials were analyzed, namely a matrix material and eight composites in which the particle volume fraction was assigned as 10% and 20% and for each the debonding property was varied in $\bar{\sigma}^{p}_{\max} = 0.5\sigma_0$, $1.5\sigma_0$, $2.5\sigma_0$ and no damage. Fig. 3 shows the influence of damage on the uniaxial stress–strain relation for the composite with $f_{p0} = 20\%$, which was also obtained by numerical calculation under strain control with a strain increment of 0.003–0.004%. It is found from Fig. 3 that the stress–strain relation is shifted upward from that of the matrix material by the reinforcing effect due to the particles as in the perfect composite, and it is shifted downward from that of the perfect composite by the debonding damage. The stress reduction due to debonding damage is more remarkable in the composite with lower debonding strength.

3.2. Finite element analysis of a crack-tip field

The numerical analyses of an edge-cracked three-point-bending specimen were carried out under plane strain condition by using a finite element method, which was developed based on the incremental damage theory of particulate-reinforced composites. The finite element method was formulated on the basis of quadrilateral 8-noded isoparametric elements with integration at four Gauss points. Fig. 4 shows the three-point-bending specimen and a finite element mesh for a half region of the specimen. In order to avoid the numerical problem for crack-tip singularity and to describe the crack-tip blunting due to the plastic deformation, a very thin notch with notch radius of 0.02 mm is regarded as a crack. The finite element mesh contains 228 elements and 759 nodes. The first step of incremental analysis was solved for linear problem up to the applied load which corresponds to the damage initiation or plastic deformation at only one Gauss point in the whole region. In the following steps, Newton–Raphson method was adopted to solve nonlinear problem for each load increment. The load increment was assigned as around one thirtieth of the remaining load from the first step load to the maximum load corresponding to general yield of the specimen (Nayak and Zienkiewicz, 1972). The elastic–plastic fracture mechanics parameter J-integral was calculated by the path-independent integral for each stage of deformation, and was expressed as $J = \_\sigma_0$ N/m using σ_0 measured in MPa.

The present FEM analyses provide us with distributions of overall macroscopic stress/strain, distributions of average microscopic stresses/strains of the matrix and particles, plastic zone due to matrix plasticity and damage zone around a crack-tip.

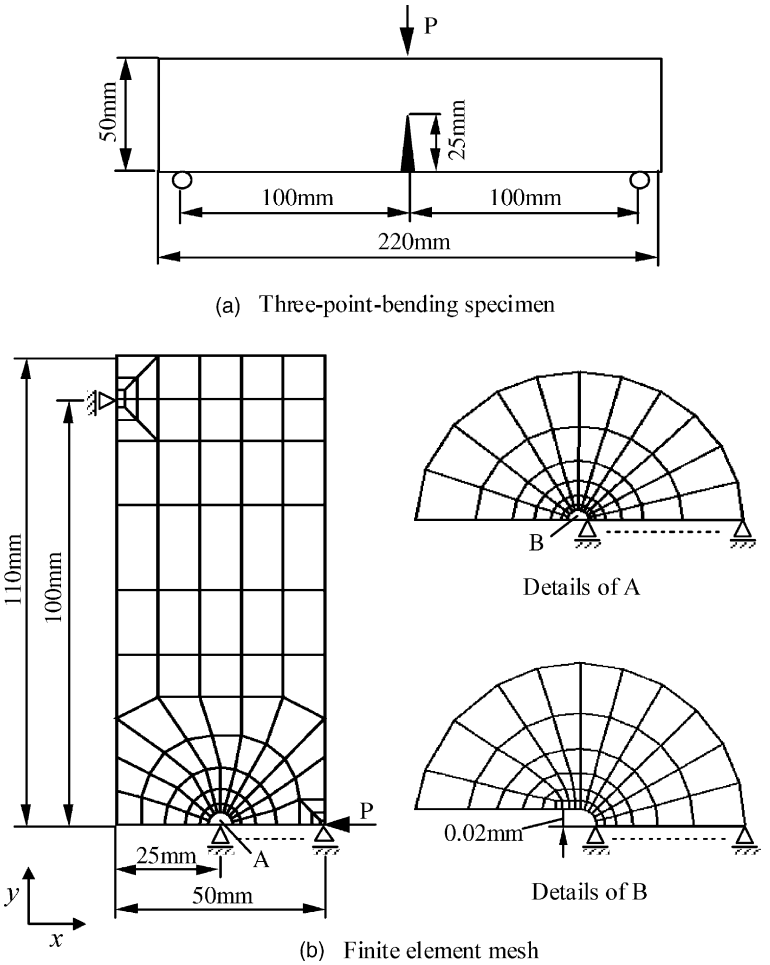

Fig. 4. Three-point-bending specimen and its finite element mesh.

4. Elastic singular field around a crack-tip

4.1. Damage evolution and stress distribution around a crack-tip

Based on the numerical results for the elastic-matrix composites, the influence of debonding damage on the elastic singular field around a crack-tip will be discussed here. Fig. 5 shows distributions of void volume fraction (damage evolution) and macroscopic equivalent stress around a crack-tip under $J = 1.01\sigma_0$ N/m for the perfect and damaged composites ($f_{p0} = 20\%$). In the composite with damage, a damage zone develops around a crack-tip. The void volume fraction increases with decreasing distance from the crack-tip and a complete damage zone where all particles are debonded is created at the vicinity of the crack-tip. From the comparison of stress distribution between the perfect and damaged composites, it is found that the equivalent stress is reduced by the debonding damage. This is caused by the stress release due to the debonding damage.

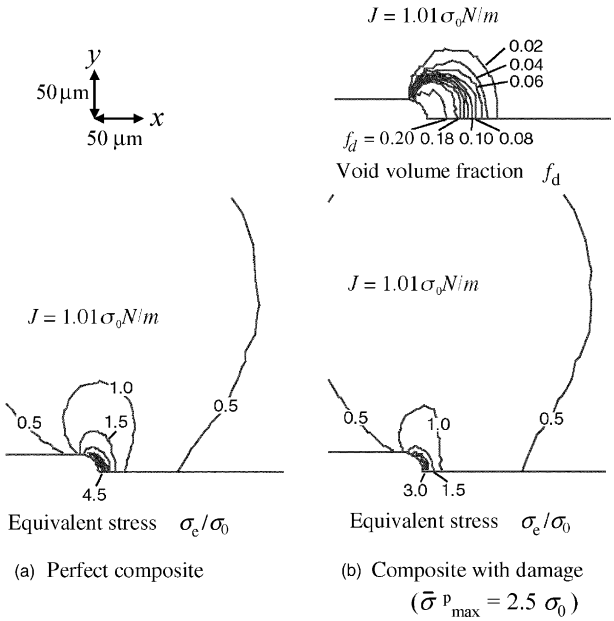

Fig. 5. Damage zone and equivalent stress around a crack-tip in elastic-matrix composites.

4.2. Stress distributions ahead of a crack-tip

Figs. 6 and 7 exhibit distributions of macroscopic stress and microscopic matrix stress along the line ahead of a crack-tip, respectively. In these figures, normalized stresses (σ_y/σ_0 and σ_y^0/σ_0) are plotted against the normalized distance ($x/(J/\sigma_0)$) from a crack-tip in a log-log diagram. The volume fraction of damaged particles is also shown for the right hand linear scale in Fig. 6. As shown in Fig. 6, the macroscopic stress distribution for the perfect composite is described by a straight line of gradient $-1/2$, i.e. the elastic singular stress field. The stress distribution for the damaged composite is characterized by the three regions with no damage, progressive damage and complete damage. The stress distribution is consistent with that for the perfect composite in the no damage zone, shifts downward in the progressive damage zone and is again described by the elastic singular stress field with a straight line of gradient $-1/2$ in the complete damage zone (Ravichandran and Liu, 1998).

Generally, the stress distribution along the line ahead of a crack-tip in elastic materials is given as

$$\frac{\sigma_y}{\sigma_0} = \frac{K_{\mathrm{I}}}{\sigma_0\sqrt{2\pi x}} = \sqrt{\frac{E}{2\pi\sigma_0(1-\nu^2)}}\frac{1}{\sqrt{x/(J/\sigma_0)}} \tag{36}$$

where E and ν are the Young's modulus and Poisson's ratio, respectively. Although the stress distribution is uniquely described by the stress intensity factor K_{I}, the stress distribution in $\sigma_y/\sigma_0 - x/(J/\sigma_0)$ diagram depends on the elastic moduli, mainly on the Young's modulus. For example, since the Young's modulus is higher in the perfect composite and lower in the porous material than that in the matrix material, the stress distribution shifts upward in the perfect composite and downward in the porous material comparing with that for the matrix material. This suggests that the stress reduction in damage zone in Fig. 6 is attributed to the change of elastic moduli due to damage because the complete damage zone corresponds to the porous material.

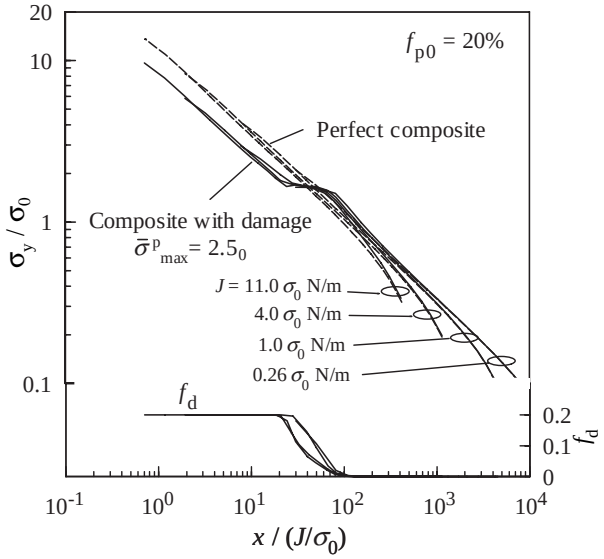

Fig. 6. Distributions of macroscopic stress and void volume fraction along the line ahead of a crack-tip in elastic-matrix composites.

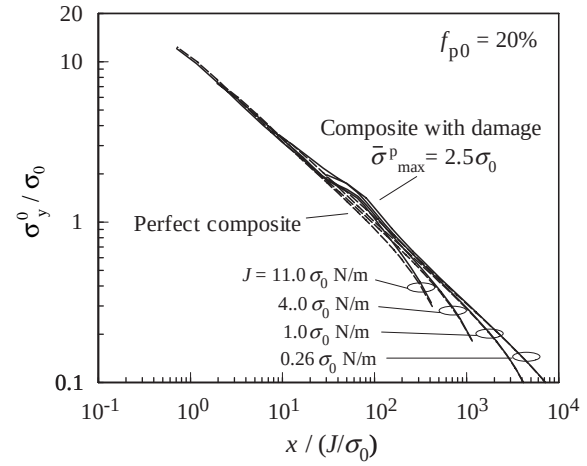

Fig. 7. Distributions of microscopic stress of the matrix along the line ahead of a crack-tip in elastic-matrix composites.

On the other hand, as shown in Fig. 7, the distributions of microscopic matrix stress in both composites are described by a unique straight line of gradient $-1/2$, namely there is no influence of debonding damage on the microscopic stress of the matrix.

According to the above results, the crack-tip field in the elastic-matrix composite with damage is described by the elastic singular field for the complete damage zone and the surrounding elastic singular field for the no damage zone as shown in Fig. 8. The stress field for the no damage zone is expressed by the stress intensity factor K_I obtained from the applied load and crack length, while the stress field for the complete damage zone is expressed by K_{Id}. Furthermore, K^0_I and K^0_{Id} can be defined to describe the stress fields due to microscopic stress of the matrix for the no damage and complete damage zones, respectively. Obviously, the

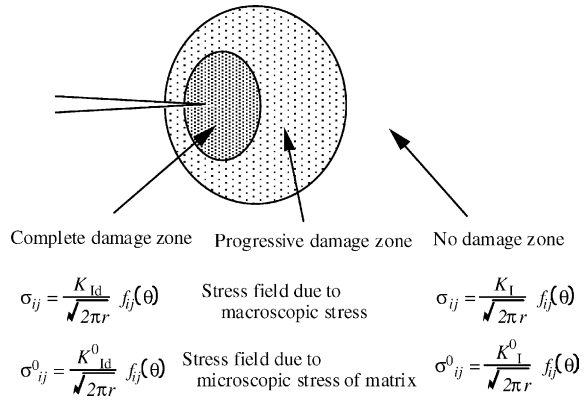

Fig. 8. Elastic stress field around a crack-tip in elastic-matrix composites with debonding damage.

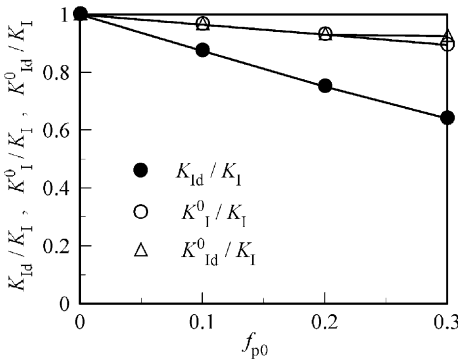

Fig. 9. Stress intensity factors of a crack-tip field in elastic-matrix composites as a function of particle volume fraction.

macroscopic stress and microscopic matrix stress fields around a crack-tip in perfect composites are described by K_I and K^0_I, respectively. These stress intensity factors were determined from the stress distributions as shown in Figs. 6 and 7, and K_{Id}/K_I, K^0_I/K_I and K^0_{Id}/K_I are plotted against the particle volume fraction f_{p0} in Fig. 9. K_{Id}/K_I decreases with an increase in f_{p0}; this means that the macroscopic stress field is considerably reduced by the debonding damage. On the other hand, K^0_I/K_I and K^0_{Id}/K_I are almost the same, and slightly decrease with an increase in f_{p0}; this means that the stress field due to the microscopic matrix stress is not affected by the debonding damage.

The influence of debonding damage on the stress fields around a crack-tip in the elastic-matrix composite can be summarized as follows. Fig. 10 schematically illustrates the stress distributions along the line ahead of a crack-tip in the perfect and damaged composites. In the perfect composite shown in Fig. 10(a), as the intact-hard particles carry the higher stress than the matrix, the relationship among the macroscopic stress σ_y and microscopic stresses in particles and matrix σ^p_y and σ^0_y is $\sigma^p_y > \sigma_y > \sigma^0_y$. σ_y and σ^0_y are described by the stress intensity factors K_I and K^0_I, respectively. In the damaged composite shown in Fig. 10(b), the macroscopic stress is reduced by the debonding damage. However, as the debonded particles can not sustain the stress, the microscopic matrix stress is higher than the macroscopic stress. σ_y and σ^0_y are described by the stress intensity factors K_{Id} and K^0_{Id}, respectively. As a result, the microscopic matrix stress in the damaged composites is close to that in the perfect composite.

The influence of damage on the macroscopic and microscopic stress fields is important in the discussion of the influence of damage on the fracture toughness of elastic-matrix composites such as ceramic-particulate-

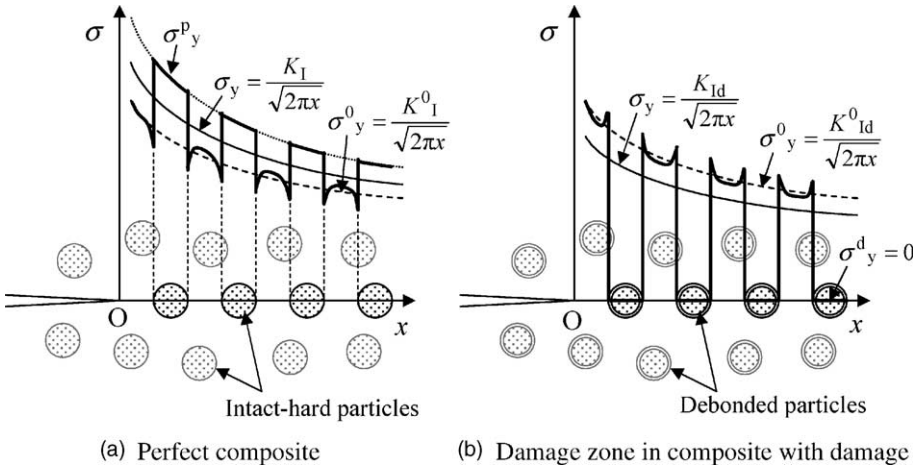

Fig. 10. Schematic illustration of the stress distributions along the line ahead of a crack-tip in perfect composite and composite with damage.

reinforced ceramic-matrix composites. The reduction of macroscopic stress by damage reminds us of the toughening due to damage. However, as the crack extension from a pre-existing crack in the composites occurs by fracture of the matrix after the debonding damage, the stress field due to microscopic stress of the matrix is more important than the macroscopic stress field. From no influence of the debonding damage on the matrix stress field, it is suggested that the toughening due to the debonding damage in the elastic-matrix composites is questionable at least from a view point of stress fields.

5. Elastic–plastic singular field around a crack-tip

5.1. Plastic zone, damage zone and equivalent stress distribution around a crack-tip

Based on the numerical results for the elastic–plastic-matrix composites, the influence of the debonding damage on the elastic–plastic singular field around a crack-tip will be discussed. Fig. 11 shows the plastic zone, void volume fraction (damage evolution) and macroscopic equivalent stress around a crack-tip in the matrix material ($f_{p0} = 0\%$), perfect composite ($f_{p0} = 20\%$) and composites with damage ($f_{p0} = 20\%$) under $J = 1.0\sigma_0$ N/m. The plastic zone indicates the region where the microscopic stress of the matrix satisfies the von Mises' yield condition. The size of plastic zone is comparable in both matrix material and perfect composite, and it tends to become large in the composites with damage. The plastic zone spreads out widely from a crack-tip after completion of debonding damage in the composites with the debonding strength of $0.5\sigma_0$ and $1.5\sigma_0$, while it develops ahead of a crack-tip with the damage evolution in the composite with $2.5\sigma_0$. The equivalent stress around a crack-tip in the perfect composite is higher than that in the matrix material, and in the composites with damage it decreases from that in the perfect composite with a decrease in the debonding strength.

5.2. Stress distributions ahead of a crack-tip

Distributions of the macroscopic stress along the line ahead of a crack-tip under four J levels are shown in Fig. 12(a) and (b). In these figures, the macroscopic stress is presented as a function of the normalized distance from a crack-tip in a log-log diagram, and distributions of void volume fraction are also shown for

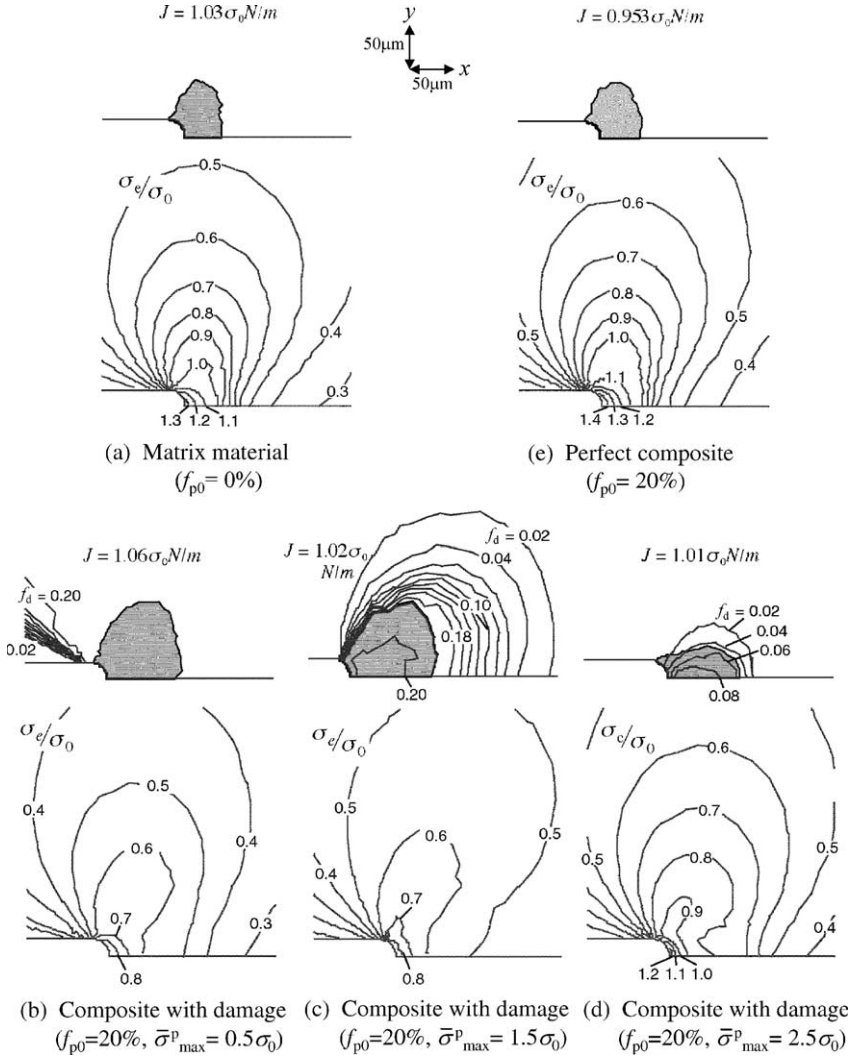

Fig. 11. Plastic zone, damage zone and equivalent stress around a crack-tip in matrix material ($f_{p0} = 0\%$) and elastic–plastic-matrix composites.

the right hand linear scale. For the elastic–plastic materials such as matrix material and perfect composites, the elastic region is described by a straight line of gradient $-1/2$ and the plastic region is described by a line of gradient $-N/(N+1)$, where N is the work-hardening exponent of each material (HRR field, Hutchinson, 1968; Rice and Rosengren, 1968). Fig. 12(a) exhibits the influence of interfacial strength on the stress distributions in the composites ($f_{p0} = 20\%$). The stress distribution in the perfect composites is higher than that in the matrix material owing to the reinforcing effect due to intact-hard particles. In the composites with damage, the stress distribution shifts downward from that for the perfect composite in the damage zone: the stress level in the damage zone goes down with a decrease in the interfacial strength. From the distributions of the stress and void volume fraction, the influence of the debonding damage on the stress distribution of the crack-tip field can be well observed. Fig. 12(b) exhibits the influence of particle volume fraction on the stress distributions in the perfect composites and composites with damage ($\bar{\sigma}^p_{\max} = 1.5\sigma_0$).

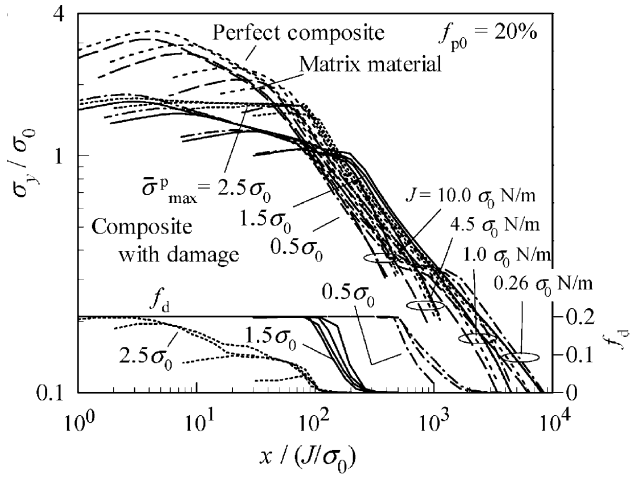

(a) Influence of interfacial strength

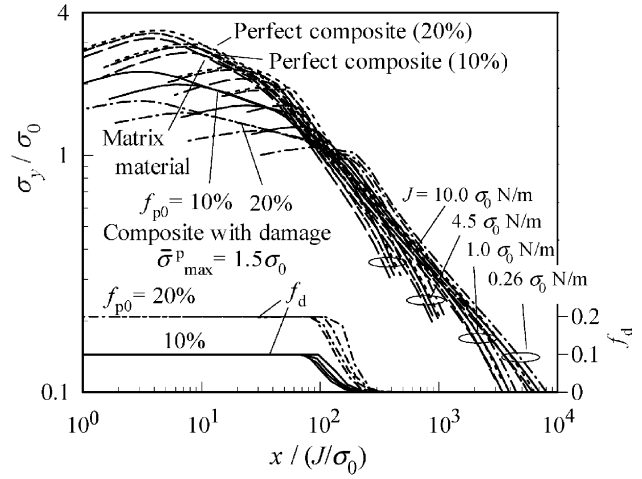

(b) Influence of particle volume fraction

Fig. 12. Distributions of macroscopic stress and void volume fraction along the line ahead of a crack-tip in elastic–plastic-matrix composites.

With increasing the particle volume fraction, the stress level around a crack-tip increases in the perfect composites and decreases in the composites with damage.

Fig. 13(a) and (b) show the distributions of the microscopic matrix stress along the line ahead of a crack-tip. From the comparison between the microscopic stress distribution (Fig. 13) and macroscopic stress distribution (Fig. 12), it is found that the influence of the debonding damage is smaller on the microscopic stress distribution than on the macroscopic stress distribution.

As mentioned in the previous section, in the elastic-matrix composites the macroscopic stress field around a crack-tip was reduced by the debonding damage while the stress field due to microscopic matrix stress was not affected by the debonding damage. In the elastic–plastic-matrix composites, however, both the macroscopic and microscopic stress fields around a crack-tip were reduced by the debonding damage. This seems to be caused by that the composite after complete damage behaves as a porous matrix material

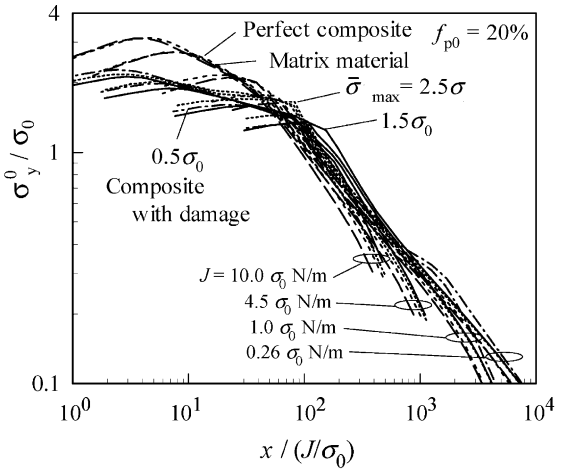

(a) Influence of interfacial strength

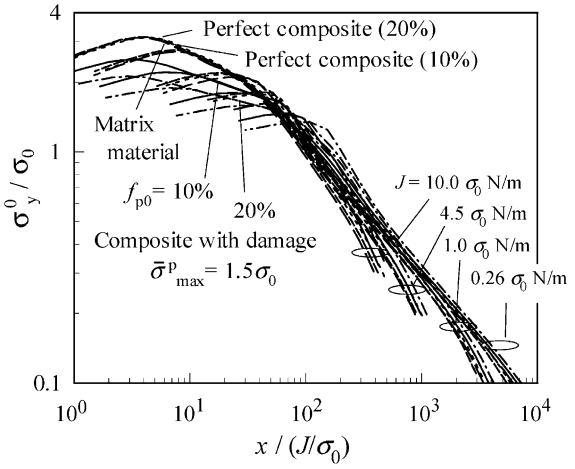

(b) Influence of particle volume fraction

Fig. 13. Distributions of microscopic stress of the matrix along the line ahead of a crack-tip in elastic–plastic-matrix composites.

and is easy to deform plastically. The reduction of microscopic stress field in the elastic–plastic-matrix composites means the toughening due to damage. It is conclusively suggested that the toughening due to damage can be expected in the elastic–plastic-matrix composites in contrast with in the elastic-matrix composites.

Fig. 14 schematically illustrates the influence of the intact-hard particles and debonding damage on the distributions of the macroscopic stress and microscopic matrix stress for the elastic–plastic-matrix composites. In Fig. 14(a), comparing with the macroscopic stress distribution of the matrix material, the perfect composite shows the high stress distribution achieved by an increase in the Young's modulus and in the yield stress due to intact-hard particles. If the debonding damage occurs around a crack-tip, the stress within the damage zone is reduced from the stress distribution for the perfect composite, and this stress reduction depends on the damage evolution. The schematic illustrations of the crack-tip field (i) and (ii) in Fig. 14 correspond to the composites with high and low interfacial strength, respectively. In the composite with high interfacial strength the damage evolves with the plastic deformation, while in the composite with

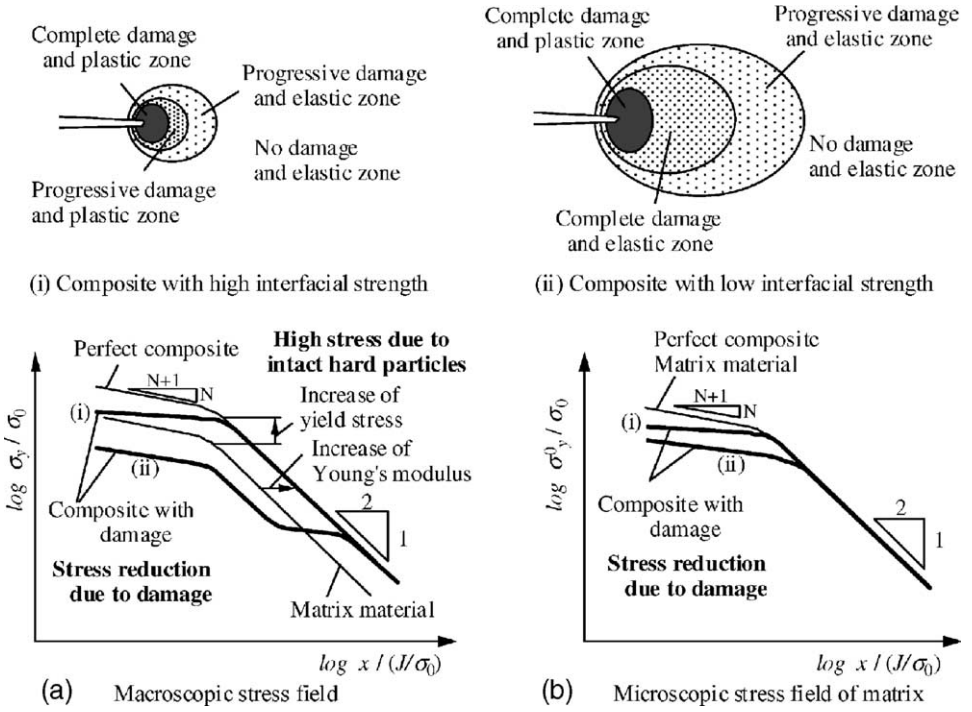

Fig. 14. Schematic illustration of the influence of intact-hard particles and debonding damage on the stress field around a crack-tip in elastic–plastic-matrix composites.

low interfacial strength the plastic deformation develops after the damage progresses and completes in the elastic zone. As shown in Fig. 14(b), the microscopic stress field is almost the same in the matrix material and perfect composite and after the damage evolution in the composite with damage it is reduced in the plastic zone but not in the elastic zone. The influence of the intact-hard particles and debonding damage on the stress fields around a crack-tip is more remarkable in the composite with higher particle content.

5.3. Influence of intact-hard particles and debonding damage on strength properties

One can estimate the effect of intact-hard particles and debonding damage on the strength of elastic–plastic-matrix composites based on the present numerical results. As shown in the numerical results of stress–strain relations, load carrying capacity of the composites is enhanced by the intact-hard particles and is reduced by the debonding damage. This suggests that the tensile strength and fatigue strength obtained by smooth specimens may be enhanced by the intact-hard particles and reduced by the debonding damage. On the other hand, since the stress level in the crack-tip field goes up by the intact-hard particles and goes down by the debonding damage as in Fig. 14, the fracture toughness and fatigue crack growth resistance may be reduced by the intact-hard particles and increased by the debonding damage. Therefore, the mechanical performance of actual composites may be obtained as a result of the competitive effects of the intact particles and the debonding damage. The experimental results on the tensile strength, fatigue strength, fracture toughness and fatigue crack growth resistance which support the present estimation were obtained for glass-particle-reinforced Nylon 66 composites (Tohgo et al., 1998).

Intact-hard particles and debonding damage may affect the fracture process in addition to the stress–strain relation and crack-tip stress field on particulate-reinforced composites. For example, the transition

of fracture morphology from brittle manner to ductile manner and the transition of crack path from straight extension to zigzag extension may be caused by the intact particles and debonding damage. The influence of the intact particles and debonding damage on the strength of the composites also comes out through such transition of the fracture process, and it may be estimated by toughening models such as crack bridging and crack front trapping (Kotoul and Vrbka, 2003; Qiao, 2003). In contrast to that, the present discussion has been carried out from a view point of the stress–strain relation and the stress fields around a crack-tip.

6. Conclusions

Numerical analyses are carried out on a crack-tip field in elastic-matrix and elastic–plastic-matrix composites reinforced with elastic particles taking account of the debonding damage of particle-matrix interface. The following conclusions are obtained:

1. On a crack-tip field in the elastic-matrix composite, there exists an elastic singular field for the complete damage zone surrounded by the conventional elastic singular field for the no damage zone. The macroscopic stress field around a crack-tip is reduced by the debonding damage while the stress field due to microscopic matrix stress is not affected by the damage.
2. A crack-tip field in the elastic–plastic-matrix composite consists of the elastic singular field and elastic–plastic singular field. Both the macroscopic and microscopic matrix stresses around a crack-tip are reduced by the debonding damage, and this reduction is more remarkable in the composite with lower interfacial strength between the particles and matrix and higher particle volume fraction.
3. From the present results it is suggested that the toughening due to debonding damage is questionable in the elastic-matrix composites while it is likely in the elastic–plastic-matrix composites.

Acknowledgement

The present work was supported by the Grant-in-Aid for Scientific Research ((B)(2) 15360050) from the Ministry of Education, Science, Sports and Culture of Japan.

References

Bao, G., 1992. Damage due to fracture of brittle reinforcements in a ductile matrix. Acta Metall. Mater. 40, 2547–2555.

Bayha, T.D., Kilmer, R.J., Wawner, F.E., 1992. The fracture characteristics of Al–9Ti/SiCp metal matrix composites. Metall. Trans. A 23, 1653–1662.

Berveiller, M., Zaoui, A., 1979. An extension of the self-consistent scheme to plastically-flowing polycrystals. J. Mech. Phys. Solids 26, 325–344.

Brencich, A., Carpinteri, A., 2000. A heuristic approach to microcracking and fracture for ceramics with statistical consideration. Theoret. Appl. Fracture Mech. 33, 135–143.

Brockenbrough, J.R., Zok, F.W., 1995. On the role of particle cracking in flow and fracture of metal matrix composites. Acta Metall. Mater. 43, 11–20.

Caceres, C.H., Griffiths, J.R., 1996. Damage by cracking of silicon particles in an Al–7Si–0.4Mg casting alloy. Acta Mater. 44, 25–33.

Charalambides, P., McMeeking, R.M., 1987. Finite element simulation of crack propagation in a brittle microcracking solid. Mech. Mater. 6, 465–472.

Chen, J.K., Huang, Z.P., Mai, Y.W., 2003. Constitutive relation of particulate-reinforced viscoelastic composite materials with debonded microvoids. Acta Mater. 51, 3375–3384.

Cho, Y.T., Tohgo, K., Ishii, H., 1997. Load carrying capacity of a broken ellipsoidal inhomogeneity. Acta Mater. 45, 4787–4795.

Dvorak, G.J., Benveniste, Y., 1992. On transformation strains and uniform fields in multiphase elastic media. Proc. R. Soc. London A 432, 291–310.
Eshelby, J.D., 1957. The determination of the elastic field of an ellipsoidal inclusion, and related problems. Proc. R. Soc. London A 241, 376–396.
Evans, A.G., Faver, K.T., 1984. Crack-growth resistance of microcracking brittle materials. J. Am. Ceram. Soc. 67, 255–260.
Finot, M., Shen, Y.L., Needleman, A., Suresh, S., 1994. Micromechanical modeling of reinforcement fracture in particle-reinforced metal-matrix composites. Metall. Mater. Trans. A 25, 2403–2420.
Gong, S.X., 1995. On the formation of near-tip microcracking and associated toughening effects. Eng. Fract. Mech. 50, 29–39.
Hartingsveldt, E.A.A., Aartsen, J.J., 1989. Interfacial debonding in polyamide-6/glass bead composites. Polymer 30, 1984–1991.
Hashin, Z., 1991. The spherical inclusion with imperfect interface. ASME J. Appl. Mech. 58, 444–449.
Hori, M., Nemat-Nasser, S., 1987. Interacting micro-cracks near the tip in the process zone of a macro-crack. J. Mech. Phys. Solids 35, 601–629.
Hutchinson, J.W., 1968. Singular behaviour at the end of a tensile crack in a hardening material. J. Mech. Phys. Solids 16, 13–31.
Hutchinson, J.W., 1987. Crack tip shielding by micro-cracking in brittle solids. Acta Metall. 35, 1605–1619.
Kachanov, M., Montagut, E.L., Laures, J.P., 1990. Mechanics of crack-microcrack interactions. Mech. Mater. 10, 59–71.
Kiser, M.T., Zok, F.W., Wilkinson, D.S., 1996. Plastic flow and fracture of a particulate metal matrix composite. Acta Mater. 44, 3465–3476.
Kotoul, M., Vrbka, J., 2003. Crack bridging and trapping mechanisms used to toughen brittle matrix composite. Theoret. Appl. Fract. Mech. 40, 23–44.
Llorca, J., Martin, A., Ruiz, J., Elices, M., 1993. Particulate fracture during deformation of a spray formed metal-matrix composite. Metall. Trans. A 24A, 1575–1588.
Llorca, J., Segurado, J., 2004. Three-dimensional multiparticle cell simulation of deformation and damage in sphere-reinforced composites. Mater. Sci. Eng. A 365, 267–274.
Matous, K., 2003. Damage evolution in particulate composite materials. Int. J. Solids Struct. 40, 1489–1503.
Mori, T., Tanaka, K., 1973. Average stress in matrix and average elastic energy of materials with misfitting inclusions. Acta Metall. 21, 571–574.
Nayak, G.C., Zienkiewicz, O.C., 1972. Elasto-plastic stress analysis. A generalization for various constitutive relations including strain softening. Int. J. Numer. Methods Eng. 5, 113–135.
Needleman, A.A., 1987. Continuum model for void nucleation by inclusion debonding. ASME J. Appl. Mech. 54, 525–531.
Ortiz, M., 1987. Continuum theory of crack shielding in ceramics. ASME J. Appl. Mech. 54, 54–58.
Ortiz, M., 1988. Microcrack coalescence and macroscopic crack growth initiation in brittle solids. Int. J. Solids Struct. 24, 231–250.
Qiao, Y., 2003. Fracture toughness of composite materials reinforced by debondable particulates. Scripta Mater. 49, 491–496.
Ravichandran, G., Liu, C.T., 1998. Crack tip shielding in elastic particulate composites undergoing damage. Eng. Fract. Mech. 59, 713–723.
Rice, J.R., Rosengren, G.F., 1968. Plane strain deformation near a crack tip in a power-law hardening material. J. Mech. Phys. Solids 16, 1–12.
Rose, L.R.F., 1986a. Microcrack interaction with a main crack. Int. J. Fracture 31, 233–242.
Rose, L.R.F., 1986b. Effective fracture toughness of microcracked materials. J. Am. Ceram. Soc. 69, 212–214.
Shum, D.K.M., Hutchinson, J.W., 1990. On toughening by microcracks. Mech. Mater. 9, 83–91.
Tandon, G.P., Weng, G.J., 1986. Stress distribution in and around spheroidal inclusions and voids at finite concentration. ASME J. Appl. Mech. 53, 511–518.
Tohgo, K., Cho, Y.T., 1999. Theory of reinforcement damage in discontinuously-reinforced composites and its application. JSME Int. J. 42, 521–529.
Tohgo, K., Chou, T.W., 1996. Incremental theory of particulate-reinforced composites including debonding damage. JSME Int. J. 39, 389–397.
Tohgo, K., Fukuhara, D., Hadano, A., 2001. The influence of debonding damage on fracture toughness and crack-tip field in glass-particle-reinforced Nylon 66 composites. Compos. Sci. Technol. 61, 1005–1016.
Tohgo, K., Fukuhara, D., Hadano, A., Ishii, H., 1998. Influence of debonding damage on mechanical performance of glass particle reinforced Nylon 66 composites. ASME Int. PVP-Vol. 374, 331–338.
Tohgo, K., Mochizuki, M., Ishii, H., 1998. Incremental damage theory and its application to glass-particle-reinforced Nylon 66 composites. Int. J. Mech. Sci. 40, 199–213.
Tohgo, K., Weng, G.J., 1994. A progressive damage mechanics in particle-reinforced metal-matrix composites under high triaxial tension. ASME J. Eng. Mater. Technol. 116, 414–420.
Whitehouse, A.F., Clyne, T.W., 1993. Cavity formation during tensile straining of particulate and short fibre metal matrix composites. Acta Metall. Mater. 41, 1701–1711.